



Evaporation of a thin film: diffusion of the vapour and Marangoni instabilities

Eric Sultan, Arezki Boudaoud, Martine Ben Amar

► To cite this version:

Eric Sultan, Arezki Boudaoud, Martine Ben Amar. Evaporation of a thin film: diffusion of the vapour and Marangoni instabilities. 2004. <hal-00002706v2>

HAL Id: hal-00002706

<https://hal.archives-ouvertes.fr/hal-00002706v2>

Submitted on 12 Nov 2004

HAL is a multi-disciplinary open access archive for the deposit and dissemination of scientific research documents, whether they are published or not. The documents may come from teaching and research institutions in France or abroad, or from public or private research centers.

L'archive ouverte pluridisciplinaire **HAL**, est destinée au dépôt et à la diffusion de documents scientifiques de niveau recherche, publiés ou non, émanant des établissements d'enseignement et de recherche français ou étrangers, des laboratoires publics ou privés.

Evaporation of a thin film: Diffusion of the vapour and Marangoni instabilities

By ERIC SULTAN, AREZKI BOUDAUD
AND MARTINE BEN AMAR

Laboratoire de Physique Statistique, Ecole Normale Supérieure, 24 rue Lhomond, 75231 Paris
Cedex 05, France

(Received 12 November 2004)

The stability of an evaporating thin liquid film on a solid substrate is investigated within lubrication theory. The heat flux due to evaporation induces thermal gradients; the generated Marangoni stresses are accounted for. Assuming the gas phase at rest, the dynamics of the vapour reduces to diffusion. The boundary condition at the interface couples transfer from the liquid to its vapour and diffusion flux. The evolution of the film is governed by a lubrication equation coupled with the Laplace problem associated with quasi-static diffusion. The linear stability of a flat film is studied in this general framework. The subsequent analysis is restricted to diffusion-limited evaporation for which the gas phase is saturated in vapour in the vicinity of the interface. The stability depends then only on two control parameters, the capillary and Marangoni numbers. The Marangoni effect is destabilising whereas capillarity and evaporation are stabilising processes. The results of the linear stability analysis are compared with the experiments of Poulard *et al.* (2003) performed in a different geometry. In order to study the resulting patterns, an amplitude equation is obtained through a systematic multiple-scale expansion. The evaporation rate is needed and is computed perturbatively by solving the Laplace problem for the diffusion of vapour. The bifurcation from the flat state is found to be a supercritical transition. Moreover, it appears that the non-local nature of the diffusion problem unusually affects the amplitude equation.

1. Introduction

Since the pioneering studies of Thomson (1855), Marangoni (1865) and Bénard (1900), much attention has been devoted to the now called Marangoni instabilities. Thomson and Marangoni first proposed surface tension gradients as a cause for convection in liquids. The Marangoni effect consists in the variation of surface tension with temperature or liquid composition and drives this class of instabilities. The hexagonal patterns observed by Bénard (1900) in thin layers heated from below prompted a number of studies (for reviews, see Davis 1987; Schatz & Neitzel 2001). Recent research in this field has focused on the correct description of the gas above the fluid layer and of the deformability of the interface (VanHook *et al.* 1997; Golovin *et al.* 1997), or the effect of local heating (Miladinova *et al.* 2002; Kalliadasis *et al.* 2003; Yeo *et al.* 2003).

Marangoni effect can also be driven by evaporation. Many experimental situations of interest are reviewed by Berg, Boudart & Acrivos (1966). On the one hand, evaporation generates thermal gradients as the phase transformation requires latent heat. For spreading droplets of slightly volatile liquids, Redon, Brochard-Wyart & Rondelez (1992)

reported festoon instabilities near the contact line while Kavehpour *et al.* (2002) measured height fluctuations over the whole drop. Hegseth, Rashidnia & Chai (1996) observed vigorous interior flow in evaporating droplets of a volatile liquid. On the other hand, in the case of mixtures, a difference of the evaporation rate between components changes the relative concentrations at the interface and so generates surface tension gradients. Fournier & Cazabat (1992); Vuilleumier, Ego, Neltner & Cazabat (1995); Fanton & Cazabat (1998); Hosoi & Bush (2001) studied tears of wine and the associated convection rolls. Nguyen & Stebe (2002) showed instabilities induced by surfactants. This composition mechanism may enhance evaporation and is therefore useful in drying techniques (Marra & Huethorst 1991; O'Brien 1993; Matar & Craster 2001).

A comprehensive theoretical stability analysis of evaporating/condensing films was done by Burelbach, Bankoff & Davis (1988). They included vapour recoil and thermocapillarity, but as in subsequent studies (see Oron *et al.* 1997; Margerit *et al.* 2003; Merkt & Bestehorn 2003), the evaporation and condensation are governed by the departure from thermodynamic equilibrium at the interface. Within this framework evaporation is intrinsically destabilising as can be seen in Prosperetti & Plesset (1984) who did not consider Marangoni stresses. In the case of very thin films (Elbaum & Lipson 1994) microscopic forces may be destabilising as shown by Samid-Merzel, Lipson & Tannhauser (1998); Lyushnin, Golovin & Pismen (2002). It is worth noticing here that all models developed in these papers are one-sided: they do not account for the gas phase dynamics except through the boundary condition at the interface.

In contrast, Deegan *et al.* (1997, 1999) showed that evaporation of pinned water droplets is limited by diffusion of vapour in air, thus they explained the origin of coffee stains. Cachile *et al.* (2002) explained their experiments on freely receding evaporating droplets within the same framework. They also observed the drops of certain fluids to lose their axisymmetry and the contact line to become wavy (Poulard *et al.* 2003). These unexplained instabilities are among the motivations of the present study. In particular, the established one-sided model would always predict an instability for evaporation.

Our aim here is to generalize the one-sided study of Burelbach *et al.* (1988) for evaporating thin films by taking into account the dynamics of the vapour. In section 2, we build a model which includes both thermodynamically determined transfer of the molecules across the interface and diffusion of vapour in the gas phase. This generalises the two class of models presented above. We describe the liquid film within lubrication theory taking into account surface tension gradients and loss of mass. In section 3, we perform the full linear stability analysis of this system. Then we restrict to the diffusion limited regime which is relevant for the experiments of Poulard *et al.* (2003). We find the amplitude equation describing patterns above the instability onset. Eventually, in section 4, we compare our results with the experiments of Poulard *et al.* (2003).

2. The model

We consider the dynamics of a two-dimensional bi-layered liquid-gas system over a solid substrate (figure 1). The gas phase is a mixture of an inert gas and of the vapour of the liquid which is volatile. We assume that the gas phase is not saturated by the vapour so that the liquid evaporates. The typical corresponding experimental situation is that of a water layer evaporating in air. The latent heat needed for the phase transformation drives a heat flux to the interface in the liquid. The induced temperature variations may generate surface tension gradients.

The model derived below is built on the lubrication approximation for the liquid layer, and accounts for surface tension variations and loss of mass through evaporation. The

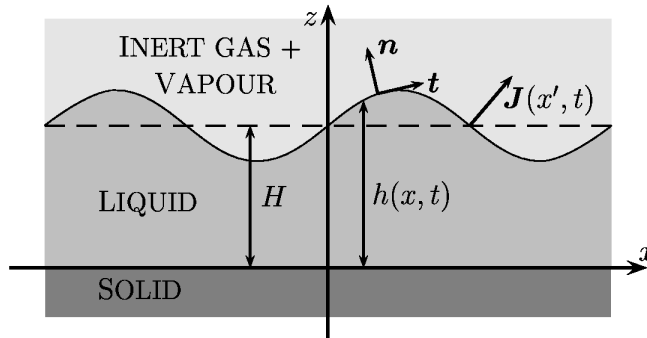


FIGURE 1. Geometry of the physical system.

gas phase is at rest; its dynamics is reduced to the diffusion of the vapour in the mixture. For a complete description of the system, the boundary conditions at the interface are needed and, in particular, the evaporation rate must be specified. Although this analysis is focused on evaporating films, it applies to the case of condensation as well.

The physical situation of interest is that of volatile liquids such as water and alkanes evaporating in air. A compilation of the physical parameters is given in table 1. The governing equations will be obtained within some approximations, which are relevant to these liquids and will be justified at the end of this section.

We restrict the study to a two dimensional system which coordinates are x along the substrate and z in the normal direction (figure 1). The state of the system is determined by the height $h(x, t)$ of the interface and the density $\rho(x, z, t)$ of vapour in the gas phase (both are functions of space and time). In the following, we write the equations describing the flow and heat diffusion in the liquid phase, diffusion in the gas phase and then the boundary conditions at the interface.

2.1. The liquid film

We consider a very thin film so that we work within the long-wavelength approximation (lubrication theory) where the typical height H is much smaller than the typical horizontal scale and we neglect gravity. Our starting point for the evolution of the thin film is a lubrication equation following Oron, Davis & Bankoff (1997)

$$\frac{\partial h}{\partial t} + \frac{\partial}{\partial x} \left\{ \frac{h^3}{3\mu} \left[\gamma \frac{\partial^3 h}{\partial x^3} + \frac{\partial}{\partial x} \left(\frac{J^2}{\rho_v} \right) \right] + \frac{h^2}{2\mu} \frac{\partial \gamma}{\partial x} \right\} = -\frac{J}{\rho_\ell} \quad (2.1)$$

where μ is the viscosity of the fluid and γ is the surface tension. The last term in the brackets comes from the shear stress due to surface tension gradients. The right-hand side corresponds to the volume loss through evaporation. ρ_ℓ is the liquid density, ρ_v the vapour density and J the mass flux across the interface. Let J_0 be the characteristic evaporation rate. The ratio $v_{\text{ev}} = J_0/\rho_\ell$ is the relevant velocity scale in the system. Vapour thrust comes from the back reaction of molecules leaving the liquid into the gas phase; it is a quadratic effect in the evaporation rate. Other forces such as Van der Waals are not included.

2.2. Surface tension gradient

To close equation (2.1) we first need to compute the surface tension gradient. We use the standard linear equation of state

$$\gamma(T) = \gamma_0 - \left| \frac{d\gamma}{dT} \right| (T - T_{\text{subs}}). \quad (2.2)$$

where $\gamma_0 = \gamma(T_{\text{subs}})$. This approximation is accurate on a large temperature range for most common liquids (not too close from a phase transition). We use the absolute value of $\frac{d\gamma}{dT}(T = T_{\text{subs}})$ as surface tension decreases with temperature for most liquids. The temperature field $T(x, z)$ satisfies the standard convection-diffusion equation in the liquid which reduces to $\frac{\partial^2 T}{\partial z^2} = 0$ in the long-wavelength approximation. Neglecting density, viscosity, thermal diffusivity and kinetic energy of the gas the energy balance at the interface gives the heat flux (Oron *et al.* 1997)

$$\kappa \frac{\partial T}{\partial z}(z = h(x)) = -\mathcal{L}_v J$$

\mathcal{L}_v being the vaporisation latent heat per unit mass, κ the thermal conductivity of the liquid. We obtain

$$T(z = h(x)) = -\frac{\mathcal{L}_v J(x)}{\kappa} h(x) + T_{\text{subs}} \quad (2.3)$$

where the substrate is assumed isothermal. Equations (2.2,2.3) result in

$$\gamma = \gamma_0 + \left| \frac{d\gamma}{dT} \right| \frac{\mathcal{L}_v}{\kappa} h J. \quad (2.4)$$

To close the system (2.1,2.4) one has to compute the evaporation rate J .

It will prove useful in the following to find an upper bound for the amplitude of the temperature variation on the interface. With the help of (2.3), we obtain: $\Delta T = \mathcal{L}_v J_0 \Delta h / \kappa$, Δh being the height fluctuations. The height fluctuations Δh are smaller than H . Thus, the reduced temperature $\frac{\Delta T}{T_{\text{subs}}}$ is bounded by $\theta = \frac{\mathcal{L}_v J_0}{\kappa} \frac{H}{T_{\text{subs}}}$, H being the characteristic thickness of the film. From table 2, we see that θ is very small for the liquids we are interested in.

2.3. The vapour

The gas phase is at rest, so that there is only diffusion of the vapour. We consider the limit of quasi-static diffusion where the characteristic diffusion time is much smaller than the characteristic evaporation time $H^2/D \ll H\rho\ell/J_0$, D being the diffusion coefficient of the vapour in the gas phase. In terms of the Péclet number $Pe = v_{\text{ev}} \frac{H}{D}$, the latter condition is $Pe \ll 1$. Hence, the vapour concentration $\rho(x, z, t)$ (local number of particles per unit volume in the gas phase) is a solution of Laplace's equation:

$$\nabla^2 \rho = 0 \quad (2.5)$$

$\nabla^2 = \frac{\partial^2}{\partial x^2} + \frac{\partial^2}{\partial z^2}$ being the 2D-Laplacian.

The gas phase is not saturated by the vapour. This condition is enforced by a constant diffusion rate at infinity

$$\frac{\partial \rho}{\partial z} \sim -\frac{J_0}{D}, \quad z \rightarrow +\infty. \quad (2.6)$$

Experimentally, either the gas is pumped at the top of the container (Mancini & Maza 2003) or the temperature of a top plate is fixed (VanHook *et al.* 1997). In both situations, the gas density is imposed at a certain height above the film, which induces a density gradient. Here, we impose the value of this gradient assuming that the height of the gas phase is much larger than other lengths in the system.

To solve (2.5) a boundary condition at the interface is needed. It is obtained in the next subsection.

2.4. Evaporation rate

The vapour and the liquid are coupled through the evaporation rate. The kinetic theory leads to a linear constitutive relation between the mass and the departure from equilibrium at the interface, known as the Hertz-Knudsen relation Prosperetti & Plesset (1984).

$$\mathbf{J}_{\text{mol}} = \alpha \sqrt{\frac{k_{\text{B}} T_{\text{int}}}{2\pi M}} (\rho_{\text{v}}^{\text{eq}}(T_{\text{int}}) - \rho|_{\text{int}}) \mathbf{n} \quad (2.7)$$

where M is the molecular weight, $\rho_{\text{v}}^{\text{eq}}$ is the density of the gas at the liquid/gas co-existence, $\rho|_{\text{int}} = \rho(z = h(x))$ is the gas density at the interface, k_{B} is the Boltzmann constant, α is the accommodation coefficient (close to unity) and \mathbf{n} is the outward normal to the interface. We note $v_{\text{th}} = \alpha \sqrt{\frac{k_{\text{B}} T_{\text{int}}}{2\pi M}}$ which is a typical kinetic velocity.

In the gas phase, the vapour mass flux, related to the departure from uniform vapour density is given by:

$$\mathbf{J} = -D \nabla \rho. \quad (2.8)$$

Due to the continuity of the normal evaporative flux at the interface, we have

$$-D(\mathbf{n} \cdot \nabla) \rho|_{\text{int}} = v_{\text{th}} (\rho^{\text{eq}}(T_{\text{int}}) - \rho|_{\text{int}}). \quad (2.9)$$

Writing a linear temperature dependant equation of state and using (2.3), one obtains for the equilibrium density at the interface:

$$\rho^{\text{eq}}(T) = \rho^{\text{eq}}(T_{\text{subs}}) - \frac{d\rho_{\text{eq}}}{dT} \frac{\mathcal{L}_{\text{v}}}{\kappa} h J.$$

Thus, the boundary condition at the interface (2.9) may be rewritten as:

$$-D \left(1 + v_{\text{th}} \frac{d\rho_{\text{eq}}}{dT} \frac{\mathcal{L}_{\text{v}}}{\kappa} h \right) (\mathbf{n} \cdot \nabla) \rho|_{\text{int}} = v_{\text{th}} (\rho^{\text{eq}}(T_{\text{subs}}) - \rho|_{\text{int}}). \quad (2.10)$$

This is a mixed boundary condition in the sense that it relates the value of the density and its normal gradient at the interface. It corresponds to the conservation of the mass i.e the equality of the evaporation rate and the mass flux in the gas. It includes both diffusion and transfer across the interface which were used separately in the literature (see subsections 2.6, 2.7 and 4.1).

2.5. Governing equations. Non dimensional parameters

For the rescaling of the equations, we choose the typical thickness H of the liquid layer, the characteristic evaporation time $H/v_{\text{ev}} = H\rho_{\ell}/J_0$, the mass flux far from the substrate J_0 and the $J_0 H/D$ as units, respectively, of length, time, evaporation rate and density of vapour in the gas phase. We make the substitutions $h \rightarrow H\tilde{h}$, $x \rightarrow H\tilde{x}$, $z \rightarrow H\tilde{z}$, $J \rightarrow \rho_{\ell} v_{\text{ev}} \tilde{J}$, $\rho \rightarrow \rho^{\text{eq}}(T_{\text{subs}}) + \tilde{\rho}(J_0 H/D)$ in equations (2.1,2.4) and (2.5,2.6,2.10). The lubrication equation becomes

$$\frac{\partial \tilde{h}}{\partial \tilde{t}} + Ca^{-1} \frac{\partial}{\partial \tilde{x}} \left\{ \frac{\tilde{h}^3}{3} \frac{\partial}{\partial \tilde{x}} \left(\frac{\partial^2 \tilde{h}}{\partial \tilde{x}^2} + \Lambda \tilde{J}^2 \right) + Ma \frac{\tilde{h}^2}{2} \frac{\partial (\tilde{h} \tilde{J})}{\partial \tilde{x}} \right\} = -\tilde{J} \quad (2.11)$$

where we have introduced $Ca = \frac{\mu v_{\text{ev}}}{\gamma_0}$, $Ma = H v_{\text{ev}} \rho_{\ell} \frac{\mathcal{L}_{\text{v}}}{\kappa} \frac{1}{\gamma_0} \left| \frac{d\gamma}{dT} \right|$ and $\Lambda = \frac{\rho_{\ell}^2 v_{\text{ev}}^2 H}{\rho_{\text{v}} \gamma_0}$ respectively the *capillary*, the *Marangoni* and the *vapour thrust* numbers. The Laplace problem reads

$$\tilde{\nabla}^2 \tilde{\rho} = \frac{\partial^2 \tilde{\rho}}{\partial \tilde{x}^2} + \frac{\partial^2 \tilde{\rho}}{\partial \tilde{z}^2} = 0 \quad (2.12)$$

	Water	Nonane	Octane	Heptane	Hexane
ρ_ℓ (kg/m ³)	1000	717	699	682	656
\mathcal{L}_v (J/kg)	$2.4 \cdot 10^6$	$3.18 \cdot 10^5$	$3.82 \cdot 10^5$	$3.21 \cdot 10^5$	$3.22 \cdot 10^5$
γ (kg/s ²)	$7.20 \cdot 10^{-2}$	$22.38 \cdot 10^{-3}$	$21.77 \cdot 10^{-3}$	$20.31 \cdot 10^{-3}$	$18.42 \cdot 10^{-3}$
μ (kg/m/s)	$8.9 \cdot 10^{-4}$	$6.65 \cdot 10^{-4}$	$5.08 \cdot 10^{-4}$	$3.87 \cdot 10^{-4}$	$3.0 \cdot 10^{-4}$
$\frac{d\rho^{\text{eq}}}{dT}$ (kg/m ³ /K)	$1.4 \cdot 10^{-3}$	$1.7 \cdot 10^{-3}$	$5.3 \cdot 10^{-3}$	$1.1 \cdot 10^{-2}$	$2.7 \cdot 10^{-2}$
$ \frac{d\gamma}{dT} $ (kg/s ² /K)	$1.5 \cdot 10^{-4}$	$9.4 \cdot 10^{-5}$	$9.53 \cdot 10^{-5}$	$9.80 \cdot 10^{-5}$	$1.02 \cdot 10^{-4}$
v_{ev} (m/s)	$0.48 \cdot 10^{-6}$	$0.2 \cdot 10^{-6}$	$0.6 \cdot 10^{-6}$	$2.2 \cdot 10^{-6}$	$6.8 \cdot 10^{-6}$
v_{th} (m/s)	148	52	55	58.8	63.3
κ (kg.m/s ³ /K)	0.60	$1.31 \cdot 10^{-1}$	$1.28 \cdot 10^{-1}$	$1.23 \cdot 10^{-1}$	$1.20 \cdot 10^{-1}$
D_{air} (m ² /s)	$1.9 \cdot 10^{-5}$	$3 \cdot 10^{-6}$	$3 \cdot 10^{-6}$	$3 \cdot 10^{-6}$	$3 \cdot 10^{-6}$

TABLE 1. Values of physical parameters for different fluids at $P = 1$ atm and $T = 25^\circ\text{C}$ (Lide 1995): liquid density ρ_ℓ , latent heat \mathcal{L}_v , surface tension γ , liquid viscosity μ , temperature derivative of gas density at equilibrium $\frac{d\rho^{\text{eq}}}{dT}$, temperature derivative of surface tension $\frac{d\gamma}{dT}$, evaporation velocity v_{ev} , thermal (kinetic) velocity v_{th} , thermal conductivity of the liquid κ and diffusion coefficient of the vapour in air D_{air} . v_{ev} is estimated from the experiments on evaporating drops Poulard *et al.* (2003) using the formula $v_{\text{ev}} = j_0/R$ where j_0 is the evaporation parameter and R is the drop radius; the diffusion coefficient in air D_{air} is roughly estimated using kinetic theory; using Clapeyron relation, we have $\frac{d\rho^{\text{eq}}}{dT} = \frac{\rho^{\text{eq}}}{P} \frac{\mathcal{L}_v}{T\Delta v} - \frac{\rho^{\text{eq}}}{T}$ where Δv is the volume change associated which the vaporization and ρ^{eq} is evaluated using the vapour pressure at saturation under 1 atm (Lide 1995).

with the two boundary conditions

$$(1 + \chi\tilde{h})(\mathbf{n} \cdot \tilde{\nabla})\tilde{\rho}|_{\text{int}} = Pe_k\tilde{\rho}|_{\text{int}} \quad \text{and} \quad \lim_{\tilde{z} \rightarrow +\infty} \frac{\partial \tilde{\rho}}{\partial \tilde{z}} = -1. \quad (2.13)$$

where $Pe_k = \frac{v_{\text{th}}H}{D}$ is a *kinetic Péclet number* and $\chi = Hv_{\text{th}} \frac{\mathcal{L}_v}{\kappa} \frac{d\rho^{\text{eq}}}{dT}$ is called the thermal expansion number.

The evaporation rate is given by

$$\tilde{J} = -(\mathbf{n} \cdot \tilde{\nabla})\tilde{\rho}|_{\text{int}} \quad (2.14)$$

which is the non dimensional version of (2.8).

2.6. The one-sided limit

The evolution equation given by Burelbach *et al.* (1988); Oron *et al.* (1997) can be recovered as a particular limit of our model. The case of no diffusion corresponds to the limit of small Pe_k . Introducing a new scaling for the density $\hat{\rho} = \tilde{\rho}Pe_k/\chi$, we find that $\hat{\rho}$ satisfies the Laplace equation (2.12) with the boundary conditions

$$\chi\tilde{J}(1 + \chi\tilde{h}) = -\hat{\rho}|_{\text{int}} \quad \text{and} \quad \lim_{\tilde{z} \rightarrow +\infty} \frac{\partial \hat{\rho}}{\partial \tilde{z}} = -\frac{Pe_k}{\chi}. \quad (2.15)$$

In the limit $Pe_k \rightarrow 0$, the boundary condition at infinity yields a uniform density distribution $\hat{\rho} = \text{Cst}$. The lubrication equation reads

$$\frac{\partial \tilde{h}}{\partial \tilde{t}} + \frac{1}{Ca} \frac{\partial}{\partial \tilde{x}} \left\{ \frac{\tilde{h}^3}{3} \frac{\partial}{\partial \tilde{x}} \left[\frac{\partial^2 \tilde{h}}{\partial \tilde{x}^2} + \Lambda \left(\frac{\chi \hat{\rho}}{1 + \chi \tilde{h}} \right)^2 \right] - Ma \frac{\tilde{h}^2}{2} \frac{\partial}{\partial \tilde{x}} \left(\frac{\chi \tilde{h} \hat{\rho}}{1 + \chi \tilde{h}} \right) \right\} = \frac{\chi \hat{\rho}}{1 + \chi \tilde{h}} \quad (2.16)$$

where J has been eliminated using (2.15). Equation (2.16) is the same as the equation obtained by Burelbach *et al.* (1988) up to a choice in scalings, when omitting the disjoining pressure term.

Number	Definition	Signification	Water	Nonane	Octane	Heptane	Hexane
Ca ($\times 10^8$)	$\frac{\mu_{ev}}{\gamma}$	$\frac{\text{viscous stresses}}{\text{capillary stresses}}$	0.6	0.6	1.4	4.2	11
Ma ($\times 10^6$)	$H \frac{\mathcal{L}_v v_{ev} \rho \ell}{\kappa \gamma} \left \frac{d\gamma}{dT} \right $	$\frac{\text{Marangoni stresses}}{\text{capillary stresses}}$	0.7	0.3	1.1	3.8	13
Pe ($\times 10^9$)	$v_{ev} \frac{H}{D}$	$\frac{\text{evaporation time}}{\text{diffusion time}}$	4.9	2.0	6.1	22	69
Pe_k	$v_{th} \frac{H}{D}$	$\frac{\text{kinetic time}}{\text{diffusion time}}$	1.5	3.5	3.7	3.9	4.2
χ	$v_{th} \frac{d\rho^{eq}}{dT} \frac{\mathcal{L}_v H}{\kappa}$	density fluctuations	0.16	0.05	0.20	0.38	1.03
$\frac{Pe_k}{\chi}$	$\frac{\kappa}{D(d\rho^{eq}/dT)\mathcal{L}_v}$	diffusion limited v.s. one-sided regime	9.4	70	18.5	10.3	4.1
θ ($\times 10^6$)	$\rho \ell v_{ev} \frac{\mathcal{L}_v}{\kappa} \frac{H}{T_{subs}}$	temperature fluctuations	1.3	0.4	1.1	4.0	12
Λ ($\times 10^{11}$)	$\frac{\rho_{ev}^2 v_{ev}^2 H}{\rho_v \gamma_0}$	$\frac{\text{vapour thrust}}{\text{capillarity}}$	2.8	0.6	1.9	9.0	31

TABLE 2. Typical values for the non-dimensional parameters.

2.7. The pure diffusion limit

We now consider the opposite limit $Pe_k \rightarrow \infty$ which we refer to as *diffusion limited regime*. The boundary conditions (2.13) for the Laplace problem (2.12) become

$$\tilde{\rho}|_{\text{int}} = 0 \quad \text{and} \quad \lim_{\tilde{z} \rightarrow +\infty} \frac{\partial \tilde{\rho}}{\partial \tilde{z}} = -1. \quad (2.17)$$

It appears that the gas is saturated in vapour immediately above the interface (in dimensional quantities, $\rho|_{\text{int}} = \rho^{eq}(T_{\text{subs}})$) and that evaporation is limited by diffusion. This boundary condition was used in the study of evaporating droplets by Deegan *et al.* (1997, 1999); Poulard *et al.* (2003); Cachile *et al.* (2002). The Laplace problem has an electrostatic equivalent: the one of finding the electric potential (ρ) with an imposed electric field (\mathbf{J}_0) at infinity and a fixed constant potential on a deformed plane. The sharp edge effect implies a larger evaporation rate at crests which tends to restore the flat state so evaporation is a stabilising mechanism in the diffusion limited regime.

2.8. Discussion

The evaluation of the relevant dimensionless parameters for water and different alkanes (table 2) shows that the limits $Pe \rightarrow 0$, $\theta \rightarrow 0$ and $\Lambda \rightarrow 0$ are reasonable. The smallness of the Péclet number Pe ensures that the time needed to build up the concentration profile above the film is much smaller than the characteristic time for the motion of the interface, so that stationary diffusion is a good approximation. The smallness of the reduced temperature θ allows a linear approximation for the gas density at the interface. The relevant physics is therefore contained in the values of the capillary, the Marangoni, the kinetic Péclet and the thermal expansion numbers (Ca , Ma , Pe_k , χ). Other mechanisms, such as molecular interactions, are neglected.

The closed system to be studied consists in the lubrication equation (2.11) coupled to a Laplace problem (2.12,2.13). This unusual coupling comes from evaporation which relates the film mass loss to the gradient of the vapour concentration. This induces non-locality in the lubrication equation as the mass loss is a function of the whole shape of the interface. To simplify notations, we drop from now on the tildes for the rescaled variables.

3. Stability of the flat interface

Equations (2.11,2.12) have as solution for the film thickness $h(x, t) = 1 - t$ and gas density $\rho(x, z, t) = -z + C - (1 - \chi/Pe_k)t$ with $C = (Pe_k - 1 - \chi)/Pe_k$. As this base state is non stationary, linearisation of the equations gives a non autonomous partial differential equation, so that standard linear stability (modal) analysis should not apply. For simplicity, we assume from now on that the base state is $h(x, t) = 1$ and $\rho(x, z, t) = -z + C$, which amounts to adding a volume source v_{ev} in the right-hand side of equation (2.1), as this source compensates exactly for the loss of mass at infinity. This also amounts to a quasi-steady approximation for which evaporation is sufficiently slow so that the thickness of the layer remains approximately constant during the growth of unstable modes.

3.1. Full linear stability analysis

We study the stability of the flat state by seeking solutions of equations (2.11,2.14) in the form:

$$h = 1 + \delta h, \quad \rho = C - z + \delta \rho, \quad J = 1 + \delta J.$$

After linearisation, those equations admit Fourier-mode solutions of wavenumber k and growth rate Ω : $\delta h = A e^{\Omega t} e^{ikx} + c.c$ (c.c stands for the complex conjugate of the preceding term); we now compute the corresponding $\delta \rho$ and δJ . To begin with, as a harmonic function, $\delta \rho$ has to be of the form $B e^{ikx} e^{-|k|z} + c.c$ (B is a complex valued function of k), where the absolute value must be taken in order to ensure vanishing $\delta \rho$ at $z \rightarrow +\infty$. The boundary condition (2.13) at the interface gives at linear order $\delta \rho|_{z=1} = \frac{Pe_k - \chi}{|k|(\chi + 1) + Pe_k} \delta h$. Hence, we can compute $B(k)$

$$\delta \rho = \frac{Pe_k - \chi}{|k|(\chi + 1) + Pe_k} \delta h e^{-|k|(z-1)} + c.c.$$

From (2.14) we get the perturbed evaporation rate $\delta J = -\frac{\partial}{\partial z} \delta \rho|_{z=1}$. Plugging in (2.11) and dropping non-linear contributions gives the dispersion relation:

$$\Omega(k) = -\frac{1}{3Ca} k^4 + \frac{Ma}{2Ca} k^2 - |k| \frac{Pe_k - \chi}{|k|(\chi + 1) + Pe_k}. \quad (3.1)$$

$\Omega(k)$ is growth rate of the wavenumber k ; if $\Omega(k) > 0$, then the perturbation grows and the corresponding mode is unstable. Evaporation can either stabilise or destabilise large wavelengths depending on the values of Pe_k and χ whereas capillarity stabilises short wavelengths; Marangoni effect drives the instability.

3.2. Transfer rate limited regime: linear stability analysis

In the limit $Pe_k \ll \min\{\chi, k, k\chi\}$, corresponding to the one-sided model, the dispersion relation (3.1) becomes

$$\Omega(k) = -\frac{1}{3Ca} k^4 + \frac{Ma}{2Ca} k^2 + \frac{\chi}{1 + \chi}. \quad (3.2)$$

meaning that the film is always unstable. This limit was studied in detail by Burelbach *et al.* (1988). In fact, it is a singular limit (the base state has a different form), and spurious effects arise at $k = 0$: equation (3.2) predicts exponential growth of a constant change in the film thickness. Accounting for the time dependance of the base state as done by Burelbach *et al.* (1988) corrects this artifact (it yields in particular $\Omega(0) = 0$) but does not change the unstable behaviour.

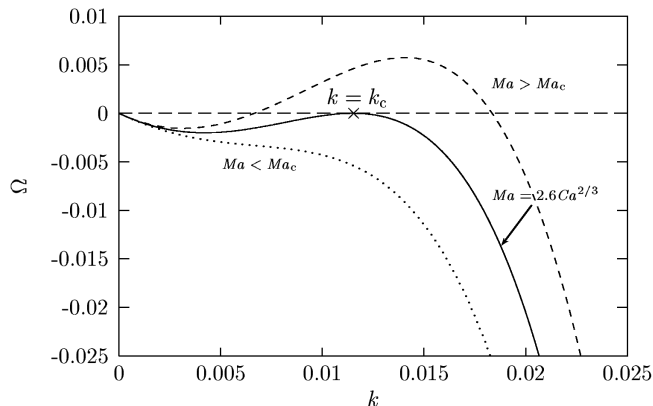


FIGURE 2. Diffusion-limited regime: growth rate Ω of the mode of wave number k (dimensionless quantities) for three typical value of the Marangoni number Ma . We have chosen here a capillary number $Ca = 10^{-6}$.

3.3. Diffusion limited regime: linear stability analysis

We now consider the opposite limit $Pe_k \gg \max\{\chi, k\}$ which is reasonable given the experimental parameters. In this regime the dispersion relation (3.1) becomes

$$\Omega(k) = -\frac{1}{3Ca}k^4 + \frac{Ma}{2Ca}k^2 - |k|. \quad (3.3)$$

The last term shows again that evaporation stabilises long wavelengths in this regime (figure 2). The absolute value of the wavenumber k comes from quasi-static diffusion. Such a non-analyticity in the dispersion relation is well-known in the context of diffusive growth (see e.g. Langer 1980). The relevant control parameters are the capillary and Marangoni numbers. Suppose that Ca is fixed; when the Marangoni number Ma is small, there is no unstable mode. The first unstable wave number k_c (marginally stable mode) appears when the Marangoni number reaches a critical value Ma_c such that $\Omega(k = k_c) = 0$ and $\frac{d}{dk}\Omega(k = k_c) = 0$. Solving this system, we obtain

$$\begin{cases} Ma_c = 18^{1/3} Ca^{2/3} \\ k_c^2 = \frac{Ma_c}{2} \end{cases} \quad (3.4)$$

for the critical parameters at the threshold.

The relevance of these results to the experiments is examined in the last section.

3.4. Diffusion limited regime: weakly non-linear analysis

The preceding linear stability analysis shows that the system may become unstable, it gives the most unstable wavelength and the instability threshold. However, predicting the nature of the transition or the observed patterns requires a more refined treatment. For instance, if the transition is discontinuous, the pattern might be very different from the linearly most unstable mode. This is why we perform a weakly nonlinear analysis close to the critical point. It is restricted to the diffusion limited regime (equations 2.11 and 2.12,2.17).

In this analysis, nonlinear contributions to the evaporation rate are needed; they are

computed in appendix A:

$$\begin{aligned}
J[h] = & 1 - \frac{\partial}{\partial x} \mathcal{H}[h] + \left\{ \frac{1}{2} \left(\frac{\partial h}{\partial x} \right)^2 + \frac{\partial^2 h}{\partial x^2} h + \frac{\partial}{\partial x} \mathcal{H} \left(h \frac{\partial}{\partial x} \mathcal{H}[h] \right) \right\} \\
& + \left\{ \frac{1}{2} \left(\frac{\partial h}{\partial x} \right)^2 \mathcal{H} \left[\frac{\partial h}{\partial x} \right] - \frac{1}{2} \frac{\partial^2}{\partial x^2} \left(h^2 \frac{\partial}{\partial x} \mathcal{H}[h] \right) - 2h \frac{\partial h}{\partial x} \mathcal{H} \left[\frac{\partial^2 h}{\partial x^2} \right] \right. \\
& \quad \left. - \frac{\partial}{\partial x} \mathcal{H} \left(h \frac{\partial}{\partial x} \mathcal{H} \left(h \frac{\partial}{\partial x} \mathcal{H}[h] \right) \right) - \frac{1}{2} \frac{\partial}{\partial x} \mathcal{H} \left[h^2 \frac{\partial^2 h}{\partial x^2} \right] \right\} \\
& + \mathcal{O}(h^4).
\end{aligned} \tag{3.5}$$

where \mathcal{H} is the Hilbert transform (appendix B). Each successive correction to the base state is an integro-differential transform of the interface profile h ; this comes from the non-local nature of the Laplace problem.

We use a multi-scale expansion which is valid when the spatial Fourier spectrum of $h(x, t)$ is concentrated around k_c (see e.g. Manneville 1990). We look for an equation of evolution for the slowly varying function $A(X, T)$ such that $h(x, t) = A(X, T) \exp(ik_c x) + \text{c.c.}$ Formally, we use ϵ as an expansion parameter. We assume that h is a function of both the fast scales x, t and the slow scales $X = \epsilon x$, $T = \epsilon^2 t$. This choice for the slow scales is the natural one given that $\Omega(k)$ is maximum at k_c . We consider the neighbourhood of the marginal stability and we rescale the control parameter as

$$\Omega(k_c) = \epsilon^2 \omega(k_c).$$

From the chain rule for differentiation, we make the replacements

$$\partial_x \rightarrow \partial_x + \epsilon \partial_X, \quad \partial_t \rightarrow \partial_t + \epsilon^2 \partial_T.$$

We also assume that h can be expanded as

$$h(x, t) = 1 + \epsilon h_1(x, t) + \epsilon^2 h_2(x, t) + \dots$$

The procedure to obtain the amplitude equation (equation for $A(X, T)$) is quite standard and is detailed in appendix C. However the present case has the peculiarity that the expansion must be pursued up to order 6 as h_1 is found to vanish. This is due to the coupling between the evaporation rate and the $k = 0$ eigenmodes of the linearised evolution operator.

Taking the rescalings $X \rightarrow X/k_c$ and $T \rightarrow T/k_c$, neglecting terms of order k_c^2 and higher which is consistent with lubrication theory, the amplitude equation reads

$$\begin{aligned}
\frac{\partial A}{\partial T} = & \sigma A + \frac{3}{2} \frac{\partial^2 A}{\partial X^2} - 2i \frac{\partial^3 A}{\partial X^3} - \frac{1}{2} \frac{\partial^4 A}{\partial X^4} - \frac{45}{8} |A|^2 A \\
& + \frac{3}{2} k_c A \left\{ \mathcal{H} \iint \left(\left\{ \sigma - \frac{\partial}{\partial T} \right\} \mathcal{H} + \frac{\partial}{\partial X} \right) |A|^2 + 2i \int \mathcal{H} \left[A \frac{\partial \bar{A}}{\partial X} \right] - 4i \mathcal{H} [|A|^2] \right\}
\end{aligned} \tag{3.6}$$

the control parameter being

$$\sigma = 2 \frac{Ca - Ca_c}{Ca_c} + \frac{3}{2} \frac{Ma - Ma_c}{Ma_c}. \tag{3.7}$$

As far as we are aware of, this non-local kind of amplitude equation has not been derived before. The non-local terms are important for large amplitude patterns or for finite size systems.

The solution $A = 0$ of the amplitude equation becomes unstable when $\sigma > 0$ (which is consistent with the linear stability). When $\sigma > 0$, there are stationary solutions of the form $A(X, T) = A_0 \exp(iQX)$ with $\sigma = 45/8 |A_0|^2 + 3/2 Q^2 + 2 Q^3 + 1/2 Q^4$. They correspond to a stationary pattern with thickness fluctuation $h(x, t) = A_0 \exp\{i(k_c +$

$Q)x\}$, which is modulated around the critical wavenumber k_c . Thus, as the prefactor of $|A|^2 A$ is negative, the transition from the flat state ($A = 0$) to a state with height fluctuations is a supercritical (continuous) pitchfork bifurcation in contrast with the studies of VanHook *et al.* (1997) or Thiele & Knobloch (2004) on heated fluid layers.

4. Discussion

4.1. Transfer rate limited versus diffusion limited evaporation

We obtained (2.9) as a boundary condition prescribed at the interface combining both the transfer rate across the interface and the diffusion of the vapour in the gas phase. This boundary condition might be simplified in two distinct limits according to the values of the kinetic Péclet number and the thermal expansion number. These two limits have been used separately in the literature; however, it has been overlooked that they fall within a general framework, although Margerit *et al.* (2003) have treated vapour diffusion in the case of no evaporation.

In the first limit, $Pe_k \ll \min\{\chi, k, k\chi\}$, the evaporation process is limited by the transfer of molecules across the interface. The diffusion of the vapour can be ignored and the classical Hertz-Knudsen (2.7) relation gives the evaporation rate. It is worth noticing here that transfer-limited evaporation is always destabilising, if the free surface undergoes a small shape perturbation, liquid portions that are closer to (resp. farther from) the substrate evaporate faster (resp. slower) and the disturbance is amplified. The so-called one-sided models for evaporating layers (Prosperetti & Plesset 1984; Burelbach *et al.* 1988; Samid-Merzel *et al.* 1998; Lyushnin *et al.* 2002; Margerit *et al.* 2003; Merkt & Bestehorn 2003) correspond to this limit as they do not consider the dynamics of the gas phase and so discard vapour diffusion.

In the second limit, $Pe_k \gg \max\{\chi, k\}$, the evaporation process is limited by the diffusion of the vapour in the gas phase. The gas phase is saturated in vapour immediately above the interface and the evaporation flux is given by the Fick relation (2.8). The electrostatic analogue of the Laplace problem for the vapour density, and the related sharp edge effect show that the evaporation rate is larger at bumps hence diffusion limited evaporation is stabilising. The study of evaporating droplets by Deegan *et al.* (1999) and Cachile, Benichou, Poulard & Cazabat (2002) fall within this approximation.

It appears that this second limit is of large validity. Indeed, the ratio Pe_k/χ which depends only on the nature of the fluid is the range 4–70 for the fluids considered here, whereas $Pe_k > 1$ (a more restrictive condition) as soon as the thickness is larger than $D/v_{th} \sim 0.1 \mu\text{m}$, which is the thickness scale determined by the diffusivity of vapour D and the thermal velocity v_{th} .

4.2. Comparison with experiments on evaporating droplets

We turn now to the experimental relevance of our analysis. Despite the number of theoretical studies on evaporating thin films, very few experiments have been conducted. Redon *et al.* (1992), Kavehpour *et al.* (2002) and Poulard *et al.* (2003) observed instabilities in the shape of evaporating droplets. In the first set of experiments (Kavehpour *et al.* 2002; Redon *et al.* 1992), the spreading of drops of silicon oils was studied. As silicon oils have a very low volatility, evaporation rate is small and the shear stress associated with the spreading is important. In the second set of experiments (Poulard *et al.* 2003) evaporation sets the velocity scale. This is why we focus on this latter set.

Poulard *et al.* (2003) studied receding evaporating drops of water and alkanes on smooth substrates. The data in tables 1 and 2 corresponds to this experimental situation. For water, heptane and hexane the drop loses its axisymmetry and develops a regular

	Ca	Ma	$Ma_c(Ca)$	Ma_c/Ma
Water	$5.90 \cdot 10^{-9}$	$6.66 \cdot 10^{-7}$	$8.59 \cdot 10^{-6}$	12.9
Nonane	$5.94 \cdot 10^{-9}$	$2.89 \cdot 10^{-7}$	$8.60 \cdot 10^{-6}$	30
Octane	$1.4 \cdot 10^{-8}$	$1.10 \cdot 10^{-6}$	$1.52 \cdot 10^{-5}$	13.8
Heptane	$4.19 \cdot 10^{-8}$	$3.76 \cdot 10^{-6}$	$3.16 \cdot 10^{-5}$	8.4
Hexane	$1.11 \cdot 10^{-7}$	$1.33 \cdot 10^{-5}$	$6.05 \cdot 10^{-5}$	4.55

TABLE 3. Values of the control parameters (Ca , Ma) for different volatile fluids and comparison with the instability threshold in the diffusion limited regime.

wavy pattern near the contact line : the height fluctuates with a well-defined wavenumber. No instabilities are observed neither with octane nor nonane. We now compare with the stability analysis in the diffusion limited regime (3.4). This comparison requires the choice of a thickness lengthscale; we retain the typical thickness of the unstable region, $h \sim 200$ nm. We estimate the typical evaporation rate in this zone using $J(r) = J_0/\sqrt{1 - (r/R)^2}$ (Deegan *et al.* 1999), R is the drop radius and r is the distance to the drop axis. In the experiments, the radius R is of order 0.5 mm and the size of the unstable zone is $R - r \sim 5$ μ m. According to table 3 droplets of all fluids are stable. However, the geometry of a droplet is different from that of a constant thickness film analysed in this paper so we cannot conclude directly on the stability. We should only compare the relative values of the ratio Ma_c/Ma between different fluids. This ratio is of order one meaning that the distance to the threshold is small. Moreover, the fluids can be sorted from the less stable to the most stable as: hexane, heptane, water, octane and nonane. This compares well with the experiments: festoon patterns have been observed with hexane, heptane and water and none with octane and nonane. However, caution should be taken with water as evaporating droplets of water have an anomalous retraction velocity (Poulard *et al.* 2003). Equation (3.4) gives as wavelengths $\lambda_{\text{Heptane}} \simeq 320$ μ m and $\lambda_{\text{Water}} \simeq 600$ μ m which are an order of magnitude larger than the experimental $\lambda_{\text{Heptane}} \simeq 50$ μ m and $\lambda_{\text{Water}} \simeq 30$ μ m. To summarize, the comparison with experiments is satisfying as we predict an instability threshold in contrast with the one-sided model (see section 3.2), and we find that the stability increases with the weight of the alkane.

4.3. Main results

In this paper, we constructed a two-sided model for evaporating thin liquid films. In order to predict quantitatively the evaporation rate, we have considered both transfer rate across the interface and diffusion of the vapour in the gas phase. The experiments of Poulard *et al.* (2003) motivated the study of the regime for which evaporation is diffusion-limited. In this context, the system describing the evolution of the height profile h couples the lubrication of the substrate by the thin film to the diffusion of its vapour in the gas phase. Using a linear stability analysis, we predicted an instability threshold and classified the stability for different liquids, in agreement with the experiments. The results of the linear stability analysis are not too far from Poulard *et al.* (2003) experiments on evaporating droplets. To push the comparison further, it would be interesting to perform experiments on extended flat films.

Moreover, the diffusion equation confers a non-local aspect to the dynamics of the film which is found to persist in the amplitude equation (3.6) established within a weakly nonlinear study. This property was unexpected and contrasts with Friedrichs & Engel (2003) results on the Rosensweig instability of magnetic fluids; it originates from the

presence of uniform profiles in the null-space of the linearised evolution operator (see appendix C).

This study suggests investigation of more complicated situations such as when both transfer rate and diffusion of the vapour are important (i.e. when Pe_k has a finite value), in the non-linear regime. As analytical extensions to the present study seem difficult, numerical computations of the complete two-sided model would allow the investigation of effects such as the non-stationary of the base state, the finite extension of the system, three dimensional patterns or the geometry of a droplet. Consequences of the non-local terms should also be interesting to further study.

We are very grateful to Anne-Marie Cazabat and Christophe Poulard for getting us interested in the stability of evaporating droplets.

Appendix A. The evaporative flux. Electrostatic analogy.

This appendix is devoted to the perturbative treatment of the Laplace problem associated with the diffusion limited regime

$$\begin{cases} \nabla^2 \rho = 0 & (z > h(x)) \\ \rho(x, h(x)) = 0 \\ \frac{\partial \rho}{\partial z}(x, z = +\infty) = -1 \end{cases}$$

where $h = h(x)$ is a given regular (bounded and differentiable) function. Precisely, the point is to compute $-(\mathbf{n} \cdot \nabla)\rho|_{z=h(x)^+}$.

A.1. Vortex sheet formalism

Using electrostatic terminology, the problem is to find the electric field \mathbf{J} immediately above a deformed charged plane. Introducing a superficial charge distribution $\rho = \sigma(x)\delta(z - h(x))$ ($\delta(z - a)$ is a Dirac mass concentrated at the point $z = a$), one can write the integral representation:

$$\mathbf{J}(x, z) = \int \sigma(x') \frac{(x - x')\mathbf{e}_x + (z - h(x'))\mathbf{e}_z}{(x - x')^2 + (z - h(x'))^2} d\ell(x') \quad (z \neq h(x)) \quad (\text{A } 1)$$

$d\ell = \sqrt{1 + \left(\frac{dh}{dx}\right)^2} dx$ being the arc-length element.

At the interface, two boundary conditions are prescribed. To begin with, according to Gauss theorem, the field has a normal discontinuity

$$(\mathbf{J}^+ - \mathbf{J}^-) \cdot \mathbf{n} = 2\pi\sigma \frac{d\ell}{dx} \quad (\text{A } 2)$$

where \mathbf{J}^+ (resp. \mathbf{J}^-) stands for the field just above (resp. below) the interface $z = h(x)$. Moreover, the tangential component has to vanish in order to fulfil the condition $\rho(x, h(x)) = 0$:

$$\mathbf{J}^+ \cdot \mathbf{t} = \mathbf{J}^- \cdot \mathbf{t} = 0 \quad (\text{A } 3)$$

Now, setting $z = h(x)$ in (A 1), one has to take the Cauchy principal value (denoted as PV) of the integral in order to get a well defined expression. This regularised integral is equal to the half-sum of \mathbf{J}^+ and \mathbf{J}^- so that the conditions (A 2, A 3) may be rewritten as:

$$\mathbf{J}^+ = \pi\sigma \sqrt{1 + \left(\frac{dh}{dx}\right)^2} + \frac{1/4}{\sqrt{1 + \left(\frac{dh}{dx}\right)^2}} \text{PV} \int \frac{\sigma(x') - \frac{dh}{dx}(x) + \phi(x, x')}{x - x' - \frac{dh}{dx}(x) + \phi(x, x')} d\ell(x') \quad (\text{A } 4)$$

and

$$\text{PV} \int \frac{\sigma(x')}{x-x'} \frac{1 + \frac{dh}{dx}(x)\phi(x, x')}{1 + \phi(x, x')^2} d\ell(x') = 0 \quad (\text{A } 5)$$

with $\phi(x, x') = \frac{h(x)-h(x')}{x-x'}$ and $J^+ = \mathbf{J}^+ \cdot \mathbf{n} = \|\mathbf{J}^+\|$.

A.2. Perturbative treatment

The general relation (A 5) implicitly gives the superficial charge σ as a function of h . Since the inversion is not possible analytically, we assume that the deflection from the flat plane h is weak; we introduce a small parameter η such as h is replaced by ηh (a possible choice is to set $\eta = \sup_x |h(x)|$) and write a perturbative expansion $\sigma = \sigma^{(0)} + \eta\sigma^{(1)} + \eta^2\sigma^{(2)} + \dots$. The $\eta = 0$ contribution corresponds to the plane interface for which the field is uniform; the boundary condition $\mathbf{J}(x, z = +\infty) = J^{(0)}\mathbf{e}_z$ readily gives $\sigma^{(0)} = J^{(0)}/\pi$. Solving (A 5) up to $\mathcal{O}(\eta^4)$, we find

$$\sigma[h] = \frac{J^{(0)}}{\pi} \left(1 + \eta^2 \left\{ \frac{1}{2} \left(\frac{dh}{dx} \right)^2 + h \frac{d^2h}{dx^2} + \frac{d}{dx} \mathcal{H} \left[h \frac{d}{dx} \mathcal{H}[h] \right] \right\} + \mathcal{O}(\eta^4) \right) \quad (\text{A } 6)$$

where \mathcal{H} is the Hilbert transform (see Appendix B).

The remaining step is simply to plug (A 6) into (A 4). Without having to compute further terms for $\sigma(x)$, we can express the evaporative flux expansion up to $\mathcal{O}(h^4)$. Setting $\eta = 1$, we find

$$\begin{aligned} J[h] = 1 - \frac{d}{dx} \mathcal{H}[h] + & \left\{ \frac{1}{2} \left(\frac{dh}{dx} \right)^2 + \frac{d^2h}{dx^2} h + \frac{d}{dx} \mathcal{H} \left(h \frac{d}{dx} \mathcal{H}[h] \right) \right\} \\ & + \left\{ \frac{1}{2} \left(\frac{dh}{dx} \right)^2 \mathcal{H} \left[\frac{dh}{dx} \right] - \frac{1}{2} \frac{d^2}{dx^2} \left(h^2 \frac{d}{dx} \mathcal{H}[h] \right) - 2h \frac{dh}{dx} \mathcal{H} \left[\frac{d^2h}{dx^2} \right] \right. \\ & \left. - \frac{d}{dx} \mathcal{H} \left(h \frac{d}{dx} \mathcal{H} \left(h \frac{d}{dx} \mathcal{H}[h] \right) \right) - \frac{1}{2} \frac{d}{dx} \mathcal{H} \left[h^2 \frac{d^2h}{dx^2} \right] \right\} \\ & + \mathcal{O}(h^4). \end{aligned}$$

that is, the formula (3.5).

Appendix B. Hilbert transform

B.1. Definition and basic properties

Given a bounded function $f(x)$, we define the Hilbert transform with the usual conventions:

$$\mathcal{H}[f](x) = \frac{1}{\pi} \lim_{\epsilon \rightarrow 0^+} \int_{|x-x'| > \epsilon} dx' \frac{f(x')}{x' - x}$$

where we have taken the Cauchy principal value (symmetric limit) at $x' = x$. Useful properties are commutation with linear differential operators and the inversion relation $\mathcal{H}^{-1} = -\mathcal{H}$. With this definition, the Hilbert transform is not defined for constant functions. However, one can remove the divergence at infinity by taking the principal values both at x and at infinity; the result is then $\mathcal{H}[\text{Cst}] = 0$. (Note that the inversion formula is not valid for constants.)

B.2. Hilbert transform and slow space varying amplitude

In the weakly non-linear analysis, we have to compute quantities of the form $\mathcal{H}[A(\epsilon x) e^{ikx}]$, with $0 < \epsilon \ll 1$. We want here to show that, up to a very good precision (for ϵ sufficiently small), we have the relation

$$\mathcal{H}[A(\epsilon x) e^{ikx}] = A(\epsilon x) \mathcal{H}[e^{ikx}] \quad (k \neq 0) \quad (\text{B1})$$

which means that the action of the Hilbert transform on a slowly modulated Fourier mode does not introduce, except if $k = 0$, non-localities (see Friedrichs & Engel 2003). In the next appendix, we make a substantial use of this property.

Since $A_\epsilon(x) = A(\epsilon x)$ varies significantly only if x has a variation of order $1/\epsilon$, the Fourier transform \hat{A}_ϵ of A_ϵ must be negligible outside of $(-\epsilon, \epsilon)$.

Let's first assume that the support of \hat{A}_ϵ (that is, the domain where it has non zero values) is included in $(-\epsilon, \epsilon)$. Then, using $\mathcal{H}[e^{ikx}] = i \operatorname{sgn}(k) e^{ikx}$ ($\operatorname{sgn}(k) = \pm 1$ if $\pm k > 0$), we have

$$\mathcal{H}[A_\epsilon(x) e^{ikx}] = i e^{ikx} \int_{-\epsilon}^{\epsilon} dk' \hat{A}_\epsilon(k') \operatorname{sgn}(k' + k) e^{ik'x}.$$

Thus, (B1) is proofed if we suppose $|k| > \epsilon$, that is, if ϵ is small enough.

If $\hat{A}_\epsilon = 0$ does not vanish outside of $(-\epsilon, \epsilon)$, one can show that, under the same hypothesis on k , to the first order in ϵ , the error on (B1) is of the order of $\int_{1/\epsilon}^{\infty} |\hat{A}(k)| dk$.

Appendix C. Weakly non linear analysis

Here we detail the weakly non linear analysis leading to the amplitude equation (3.6). We consider the neighbourhood of the stability limit, so that we rescale the control parameter according to

$$\Omega(k_c) = \epsilon^2 \omega(k_c). \quad (\text{C1})$$

Plugging (3.5) into the lubrication equation (2.11), we obtain a closed integro-differential equation for the height profile h . We assume that h is a function of x, X, t, T (fast and slow scales) and admits the expansion $h = \epsilon h^{(1)} + \epsilon^2 h^{(2)} + \dots$. The derivatives are substituted according to

$$\partial_x \rightarrow \partial_x + \epsilon \partial_X, \quad \partial_t \rightarrow \partial_t + \epsilon^2 \partial_T. \quad (\text{C2})$$

It is convenient to separate the evolution operator into its linear contributions \mathcal{L} and non-linear ones \mathcal{N} . In particular, applying transformations (C2) leads to the expansion $\mathcal{L} = \mathcal{L}_c + \epsilon \mathcal{L}^{(1)} + \epsilon^2 \mathcal{L}^{(2)} + \epsilon^3 \mathcal{L}^{(3)} + \epsilon^4 \mathcal{L}^{(4)}$ with

$$\begin{aligned} \mathcal{L}_c &= \frac{1}{3Ca} \partial_x^4 + \frac{Ma}{2Ca} (\partial_x^2 - \partial_x^3 \mathcal{H}) - \partial_x \mathcal{H}, \\ \mathcal{L}^{(1)} &= \left\{ \frac{4}{3Ca} \partial_x^3 + \frac{Ma}{2Ca} (2\partial_x - 3\partial_x^2 \mathcal{H}) - \mathcal{H} \right\} \partial_X, \\ \mathcal{L}^{(2)} &= \left\{ \frac{2}{Ca} \partial_x^2 + \frac{Ma}{2Ca} (1 - 3\partial_x \mathcal{H}) \right\} \partial_X^2 - \omega(k_c) + \partial_T, \\ \mathcal{L}^{(3)} &= \left\{ \frac{4}{3Ca} \partial_x - \frac{Ma}{2Ca} \mathcal{H} \right\} \partial_X^3, \\ \mathcal{L}^{(4)} &= \frac{1}{3Ca} \partial_X^4. \end{aligned}$$

Note that the null-space of \mathcal{L}_c contains slow space varying height profiles (i.e. functions of X). We now proceed to the solution order by order.

Order ϵ^1 :

We have simply:

$$\mathcal{L}_c h^{(1)} = 0. \quad (\text{C } 3)$$

Using (B1), the solution is

$$h^{(1)} = (A_{11}(X, T) e^{ik_c x} + \text{c.c.}) + A_{10}(X, T)$$

k_c being the critical wavenumber given by the linear stability analysis.

Order ϵ^2 :

The equation has the form

$$\mathcal{L}_c h^{(2)} = -\mathcal{L}^{(1)} h^{(1)} - \mathcal{N}^{(2)}(h^{(1)}) \quad (\text{C } 4)$$

The non-linear term contains a $k = 0$ mode. As the right-hand side of (C4) must be orthogonal to the null space of \mathcal{L}_c , it implies $h^{(1)} = 0$. Thus, $\mathcal{L}_c h^{(2)} = 0$, hence $h^{(2)} = (A_{21}(X, T) e^{ik_c x} + \text{c.c.}) + A_{20}(X, T)$.

Order ϵ^3 :

$\mathcal{N}^{(3)} = 0$ as $h^{(1)} = 0$:

$$\mathcal{L}_c h^{(3)} = -\mathcal{L}^{(1)} h^{(2)}. \quad (\text{C } 5)$$

Again, right-hand side of (C5) has to be orthogonal to the null space of \mathcal{L}_c , so we have $A_{20} = 0$. Hence, $h^{(3)} = (A_{31}(X, T) e^{ik_c x} + \text{c.c.}) + A_{30}(X, T)$.

Order ϵ^4 :

$$\mathcal{L}_c h^{(4)} = -\mathcal{L}^{(2)} h^{(2)} - \mathcal{L}^{(1)} h^{(3)} - \mathcal{N}^{(4)}(h^{(2)}). \quad (\text{C } 6)$$

The non linear term is:

$$\mathcal{N}^{(4)}(h^{(2)}) = (f_4 A_{21}^2 e^{2ik_c x} + \text{c.c.}) - k_c^2 A_{21} \overline{A_{21}}$$

with $\overline{A_{21}}$ is the complex conjugate of A_{21})

$$f_4(k_c) = \frac{Ma}{Ca} (-2k_c^2 - k_c^4 - 4k_c^3) + \frac{2k_c^4}{Ca} + \frac{1}{2}k_c^2.$$

So, introducing $\alpha = (-\frac{2}{Ca} k_c^2 + \frac{Ma}{2Ca} (1 + 3k_c))$, we have from (C6)

$$-\partial_X \mathcal{H}[A_{30}] = k_c^2 |A_{21}|^2, \quad (\text{C } 7)$$

$$-\omega(k_c) A_{21} + \alpha \partial_X^2 A_{21} + \partial_T A_{21} = 0. \quad (\text{C } 8)$$

The solution to (C6) is

$$h_4 = (A_{42}(X, T) e^{2ik_c x} + \text{c.c.}) + (A_{41}(X, T) e^{ik_c x} + \text{c.c.}) + A_{40}(X, T)$$

with $A_{42} = \frac{f_4(k_c)}{\Omega(2k_c)} A_{21}^2$.

Order ϵ^5 :

$$\mathcal{L}_c h^{(5)} = -\mathcal{L}^{(3)} h^{(2)} - \mathcal{L}^{(2)} h^{(3)} - \mathcal{L}^{(1)} h^{(4)} - \mathcal{N}^{(5)}(h^{(2)}, h^{(3)}). \quad (\text{C } 9)$$

It is convenient to decompose the non-linear term:

$$\mathcal{N}^{(5)}(h^{(2)}) = (\mathcal{N}_{52} e^{2ik_c x} + \text{c.c.}) + (\mathcal{N}_{51} e^{ik_c x} + \text{c.c.}) + \mathcal{N}_{50},$$

where

$$\begin{aligned}\mathcal{N}_{52} &= f_5 A_{31} A_{21} + i g_5 \partial_X A_{21}^2 \\ \mathcal{N}_{51} &= j_5 A_{30} A_{21} \\ \mathcal{N}_{50} &= -k_c^2 A_{21} \overline{A_{31}} - i k_c A_{21} \partial_X \overline{A_{21}} - k_c \mathcal{H} [\overline{A_{21}} \partial_X A_{21}] + \text{c.c.}\end{aligned}$$

and with

$$\begin{aligned}f_5(k_c) &= \frac{Ma}{Ca} (-8k_c^3 - 2k_c^4 - 4k_c^2) + \frac{4k_c^4}{Ca} + k_c^2 \\ g_5(k_c) &= \frac{Ma}{Ca} (2k_c + 2k_c^3 + 6k_c^2) - \frac{4k_c^3}{Ca} - \frac{k_c}{2} \\ j_5(k_c) &= \frac{Ma}{Ca} \left(-\frac{3}{2}k_c^3 - k_c^2 \right) + \frac{k_c^4}{Ca}.\end{aligned}$$

Imposing again that the restriction of the right-hand side of (C 9) to the null space of \mathcal{L}_c has to vanish and using (C 7), we get

$$i\beta \partial_X^3 A_{21} + \{ \alpha \partial_X^2 - \omega(k_c) + \partial_T \} A_{31} + j_5 A_{21} \int \mathcal{H}[|A_{21}|^2] = 0 \quad (\text{C } 10)$$

and

$$\partial_X \mathcal{H}[A_{40}] = (-\omega(k_c) + \partial_T) A_{30} + \frac{Ma}{2Ca} \partial_X^2 A_{30} + \mathcal{N}_{50}. \quad (\text{C } 11)$$

with $\beta = \frac{4}{3Ca} k_c - \frac{Ma}{2Ca}$.

The solution at this order is

$$h_5 = (A_{52}(X, T) e^{2ik_c x} + \text{c.c.}) + (A_{51}(X, T) e^{ik_c x} + \text{c.c.}) + A_{50}(X, T)$$

with $A_{52} = \frac{1}{\Omega(2k_c)} (\mathcal{N}_{52} + i\Omega'(2k_c) \partial_X A_{42})$.

Even if (C 10) is non-linear in A_{21} , it does not give the nature of the bifurcation. This is why we carry on computations to next order.

Order ϵ^6 :

$$\mathcal{L}_c h^{(6)} = -\mathcal{L}^{(4)} h^{(2)} - \mathcal{L}^{(3)} h^{(3)} - \mathcal{L}^{(2)} h^{(4)} - \mathcal{L}^{(1)} h^{(5)} - \mathcal{N}^{(6)}(h^{(2)}, h^{(3)}, h^{(4)}). \quad (\text{C } 12)$$

We only need the part of $\mathcal{N}^{(6)}$ of wavenumber k_c :

$$\begin{aligned}\mathcal{N}_{61} &= f_6 \overline{A_{21}} A_{42} + g_6 A_{21} \partial_X \mathcal{H} A_{30} + i j_6 A_{21} \partial_X A_{30} \\ &\quad + \ell_6 (A_{21} A_{40} + A_{31} A_{30}) + m_6 |A_{21}|^2 A_{21} + i n_6 A_{30} \partial_X A_{21}\end{aligned}$$

with

$$\begin{aligned}f_6(k_c) &= \frac{Ma}{Ca} \left(-k_c^2 - \frac{9}{2}k_c^3 \right) + \frac{7k_c^4}{Ca} \\ g_6(k_c) &= \frac{Ma}{Ca} \left(\frac{1}{2}k_c^3 + \frac{1}{2}k_c^2 \right) - k_c \\ j_6(k_c) &= 2\frac{Ma}{Ca} (k_c^3 + k_c^2 + k_c) - \frac{k_c^3}{Ca} \\ \ell_6(k_c) &= -\frac{Ma}{Ca} \left(\frac{3}{2}k_c^3 + k_c^2 \right) + \frac{k_c^4}{Ca} = j_5(k_c) \\ m_6(k_c) &= \frac{Ma}{Ca} \left(\frac{7}{4}k_c^5 - \frac{1}{2}k_c^2 - \frac{3}{4}k_c^4 - \frac{5}{2}k_c^3 \right) - \frac{7k_c^3}{2} + \frac{k_c^4}{Ca} \\ n_6(k_c) &= \frac{Ma}{Ca} \left(\frac{9}{2}k_c^2 + 2k_c \right) - \frac{4k_c^3}{Ca}\end{aligned}$$

After solving equations (C 7, C 11) for A_{30} and A_{40} , we use the solvability condition that the right-hand side of (C 12) is orthogonal to the null space of \mathcal{L}_c and we obtain an equation for A_{41} . Introducing

$$A = \epsilon A_{11} + \epsilon^2 A_{21} + \epsilon^3 A_{31} + \epsilon^4 A_{41} + \dots,$$

the last equation for A_{41} can be re-summed with equations (C 8,C 10) for A_{21} and A_{31} . Using the inverse transformations of (C 1,C 2), we finally obtain the amplitude equation for $A(X, T)$:

$$\begin{aligned} & (-\Omega(k_c) + \alpha\partial_X^2 + \partial_T)A + i\beta\partial_X^3 A + \frac{1}{3Ca}\partial_X^4 A + \xi|A|^2 A \\ & + ik_c(j_6 k_c - \ell_6)\mathcal{H}[|A|^2]A + in_6 k_c^2(\partial_X A) \int \mathcal{H}[|A|^2] \\ & + \ell_6 \left\{ k_c^2 A \iint (-\Omega(k_c) + \partial_T + \partial_X \mathcal{H})|A|^2 + 2ik_c A \int \mathcal{H}[A\partial_X \bar{A}] \right\} = 0. \end{aligned}$$

with

$$\xi(k_c) = m_6 + \frac{1}{\Omega(2k_c)} f_6 f_{22} - k_c^2 g_6 + \left(k_c^2 \frac{Ma}{2Ca} - 2k_c \right) \ell_6.$$

Taking the limit of small k_c with the help of the rescaling $\partial_X \rightarrow k_c \partial_X$ and $\partial_T \rightarrow k_c \partial_T$ leads to

$$\begin{aligned} & \left(\frac{\partial}{\partial T} - \sigma - \frac{3}{2} \frac{\partial^2}{\partial X^2} \right) A + 2i \frac{\partial^3 A}{\partial X^3} + \frac{1}{2} \frac{\partial^4 A}{\partial X^4} + \frac{45}{8} |A|^2 A + i6k_c \mathcal{H}[|A|^2] A + \\ & - \frac{3}{2} k_c \left\{ A \iint \left(\frac{\partial}{\partial T} - \sigma + \frac{\partial}{\partial X} \mathcal{H} \right) |A|^2 + 2iA \int \mathcal{H} \left[A \frac{\partial \bar{A}}{\partial X} \right] \right\} + \mathcal{O}(k_c^2) = 0, \end{aligned} \tag{C 13}$$

hence the simplification (3.6). Note that (C 13) is valid only if $A(X, T)$ vanishes at $X = \pm\infty$, so that Hilbert transforms \mathcal{H} are well defined. In contrast with standard weakly non-linear analysis, this equation is non-local.

REFERENCES

- BÉNARD, H. 1900 Les tourbillons cellulaires dans une nappe liquide. *Rev. Gén. Sci. Pures Appl.* **11**, 1261–1276.
- BERG, J. C., BOUDART, M. & ACRIVOS, A. 1966 Natural convection in pools of evaporating liquids. *J. Fluid Mech.* **24**, 721–735.
- BURELBACH, J. P., BANKOFF, S. G. & DAVIS, S. H. 1988 Nonlinear stability of evaporating/condensing liquid film. *J. Fluid Mech.* **195**, 463–494.
- CACHILE, M., BENICHO, O., POULARD, C. & CAZABAT, A. M. 2002 Evaporating droplets. *Langmuir* **18** (21), 8070–8078.
- DAVIS, S. H. 1987 Thermocapillary instabilities. *Annu. Rev. Fluid Mech.* **19**, 403–435.
- DEEGAN, R. D., BAKAJIN, O., DUPONT, T. F., HUBER, G., NAGEL, S. R. & WITTEN, T. A. 1997 Capillary flow as the cause of ring stains from dried liquid drops. *Nature* **389**, 827–829.
- DEEGAN, R. D., BAKAJIN, O., DUPONT, T. F., HUBER, G., NAGEL, S. R. & WITTEN, T. A. 1999 Contact line deposit in an evaporating drop. *Phys. Rev. E* **62** (1), 217–239.
- ELBAUM, M. & LIPSON, S. G. 1994 How Does a Thin Wetted Film Dry Up? *Phys. Rev. Lett.* **72** (22).
- FANTON, X. & CAZABAT, A. M. 1998 Spreading and instabilities induced by a soluted Marangoni effect. *Langmuir* **14**, 2554–2561.
- FOURNIER, J. B. & CAZABAT, A. M. 1992 Tears of wine. *Europhys. Lett.* **20**, 517–524.
- FRIEDRICH, R. & ENGEL, A. 2003 Nonlinear analysis of the Rosensweig instability. *Europhys. Lett.* **63** (6), 826–832.
- GOLOVIN, A. A., NEPOMNYASHCHY, A. A. & PISMEN, L. M. 1997 Nonlinear evolution and secondary instabilities of Marangoni convection in a liquid-gas system with deformable interface. *J. Fluid Mech.* **341**, 317–341.
- HEGSETH, J. J., RASHIDNIA, N. & CHAI, A. 1996 Natural convection in droplet evaporation. *Phys. Rev. E* **54** (2).

- HOSOI, A. E. & BUSH, W. M. 2001 Evaporative instabilities in climbing films. *J. Fluid Mech.* **442**, 217–239.
- KALLIADASIS, S., KIYASHKO, A. & DEMEKHIN, E. A. 2003 Marangoni instability of a thin liquid film heated from below by a local heat source. *J. Fluid Mech.* **475**, 377–408.
- KAVEHPOUR, P., OVRYN, B. & MCKINLEY, G. H. 2002 Evaporatively-driven Marangoni instabilities of volatile liquid spreading on thermally conductive substrates. *Colloid Surface A.* **206**, 409–423.
- LANGER, J. S. 1980 Pattern formation in crystal growth. *Rev. Mod. Phys.* **52** (1), 1–28.
- LIDE, S. R. 1995 *Handbook of Chemistry and Physics*, 75th edn. CRC Press.
- LYUSHNIN, A. V., GOLOVIN, A. A. & PISMEN, L. M. 2002 Fingering instability of thin evaporating liquid films. *Phys. Rev. E* **65**.
- MANCINI, H. & MAZA, D. 2003 Pattern formation without heating in an evaporative convection experiment. *Europhys. Lett.* **66** (6), 1–7.
- MANNEVILLE, P. 1990 *Dissipative structures and weak turbulence*. Academic Press.
- MARANGONI, C. 1865 *On the expansion of a drop of liquid floating on the surface of another liquid*. Pavia: Tipografia dei fratelli Fusi.
- MARGERIT, J., COLINET, P., LEBON, G., IORIO, C. S. & LEGROS, J. C. 2003 Interfacial nonequilibrium and Bénard-Marangoni instability of a liquid vapor system. *Phys. Rev. E* **68**.
- MARRA, J. & HUETHORST, J. A. M. 1991 Physical Principles of Marangoni Drying. *Langmuir* **7**, 2748–2755.
- MATAR, O. K. & CRASTER, R. V. 2001 Models for Marangoni Drying. *Phys. Fluids* **13**, 1869–1883.
- MERKT, D. & BESTEHORN, M. 2003 Bénard-Marangoni convection in a strongly evaporating fluid. *Physica D* **185**, 196–208.
- MILADINOVA, S., SLAVTCHEV, S., LEBON, G. & LEGROS, J. C. 2002 Long-wave instabilities of non-uniformly heated falling films. *J. Fluid Mech.* **453**, 153–175.
- NGUYEN, V. X. & STEBE, K. J. 2002 Patterning of small particles by a surfactant-enhanced Marangoni-Bénard instability. *Phys. Rev. E* **88** (16).
- O'BRIEN, S. B. G. M. 1993 On Marangoni drying: nonlinear kinematic waves in a thin film. *J. Fluid Mech.* **254**, 649–670.
- ORON, A., DAVIS, S. H. & BANKOFF, S. G. 1997 Long-scale evolution of thin liquid films. *Rev. Mod. Phys.* **69** (3), 931–980.
- POULARD, C., BENICHO, O. & CAZABAT, A. M. 2003 Freely receding evaporating droplets. *Langmuir* **19** (21), 8828–8834.
- PROSPERETTI, A. & PLESSET, M. S. 1984 The stability of an evaporating liquid surface. *Phys. Fluid* **27**, 1590–1602.
- REDON, C., BROCHARD-WYART, F. & RONDELEZ, F. 1992 Festoon instabilities of slightly volatile liquids during spreading. *J. Phys. II* **2** (9), 1671–1676.
- SAMID-MERZEL, N., LIPSON, S. G. & TANNHAUSER, D. S. 1998 Pattern formation in drying water films. *Phys. Rev. E* **57** (3).
- SCHATZ, M. F. & NEITZEL, G. P. 2001 Experiments on thermocapillary instabilities. *Annu. Rev. Fluid Mech.* **33**, 93–129.
- THIELE, U. & KNOBLOCH, E. 2004 Thin liquid films on a slightly inclined heated plate. *Physica D* **190**, 213–248.
- THOMSON, J. 1855 On certain curious motions observable at the surfaces of wine and other alcoholic liquors. *Phil. Mag.* **10**, 330.
- VANHOOK, S., SCHATZ, M., SCHATZ, M. F., SWIFT, J. B., MCCORMICK, W. D. & SWINNEY, H. L. 1997 Long-wavelength surface-length-driven Bénard convection: experiment and theory. *J. Fluid Mech.* **345**, 45–78.
- VUILLEUMIER, R., EGO, V., NELTNER, L. & CAZABAT, A. M. 1995 Tears of wine: the stationary state. *Langmuir* **11**, 4117–4121.
- YEO, L. Y., CRASTER, R. V. & MATAR, O. K. 2003 Marangoni instability of a thin liquid film on a locally heated horizontal wall. *Phys. Rev. E* **67**.